



Contents lists available at ScienceDirect

## Journal of Environmental Management

journal homepage: [www.elsevier.com/locate/jenvman](http://www.elsevier.com/locate/jenvman)

## Research article

## Rapid prediction of particulate, humus and resistant fractions of soil organic carbon in reforested lands using infrared spectroscopy



Dinesh B. Madhavan<sup>a,\*</sup>, Jeff A. Baldock<sup>b</sup>, Zoe J. Read<sup>c</sup>, Simon C. Murphy<sup>a</sup>,  
Shaun C. Cunningham<sup>d,e</sup>, Michael P. Perring<sup>f,g</sup>, Tim Herrmann<sup>h</sup>, Tom Lewis<sup>i</sup>,  
Timothy R. Cavagnaro<sup>j</sup>, Jacqueline R. England<sup>k</sup>, Keryn I. Paul<sup>l</sup>, Christopher J. Weston<sup>m</sup>,  
Thomas G. Baker<sup>a</sup>

<sup>a</sup> School of Ecosystem and Forest Sciences, The University of Melbourne, Richmond, VIC 3121, Australia

<sup>b</sup> CSIRO Agriculture, Glen Osmond, SA 5064, Australia

<sup>c</sup> Fenner School of Environment and Society, Australian National University, Acton, ACT 2601, Australia

<sup>d</sup> School of Life and Environmental Sciences, Deakin University, Burwood, VIC 3125, Australia

<sup>e</sup> Institute for Applied Ecology, University of Canberra, Bruce, ACT 2617, Australia

<sup>f</sup> School of Biological Sciences, The University of Western Australia, Crawley, WA 6009, Australia

<sup>g</sup> Forest & Nature Laboratory, Ghent University, BE-9090, Gontrode-Melle, Belgium

<sup>h</sup> Department of Environment, Water and Natural Resources, Adelaide, SA 5001, Australia

<sup>i</sup> Agri-Science Queensland, Department of Agriculture and Fisheries, Sippy Downs, QLD 4556, Australia

<sup>j</sup> School of Agriculture, Food and Wine, University of Adelaide, Waite Campus, PMB 1, Glen Osmond, SA 5064, Australia

<sup>k</sup> CSIRO Agriculture and CSIRO Land and Water, Clayton South, VIC 3169, Australia

<sup>l</sup> CSIRO Agriculture and CSIRO Land and Water, Canberra, ACT 2601, Australia

<sup>m</sup> School of Ecosystem and Forest Sciences, The University of Melbourne, Creswick, VIC 3363, Australia

## ARTICLE INFO

## Article history:

Received 21 July 2016

Received in revised form

4 February 2017

Accepted 7 February 2017

## Keywords:

C sequestration

Biodiverse environmental plantings

Mid-infrared spectroscopy

Near-infrared spectroscopy

NMR spectroscopy

Partial least squares regression

## ABSTRACT

Reforestation of agricultural lands with mixed-species environmental plantings can effectively sequester C. While accurate and efficient methods for predicting soil organic C content and composition have recently been developed for soils under agricultural land uses, such methods under forested land uses are currently lacking. This study aimed to develop a method using infrared spectroscopy for accurately predicting total organic C (TOC) and its fractions (particulate, POC; humus, HOC; and resistant, ROC organic C) in soils under environmental plantings. Soils were collected from 117 paired agricultural-reforestation sites across Australia. TOC fractions were determined in a subset of 38 reforested soils using physical fractionation by automated wet-sieving and <sup>13</sup>C nuclear magnetic resonance (NMR) spectroscopy. Mid- and near-infrared spectra (MNIRS, 6000–450 cm<sup>-1</sup>) were acquired from finely-ground soils from environmental plantings and agricultural land. Satisfactory prediction models based on MNIRS and partial least squares regression (PLSR) were developed for TOC and its fractions. Leave-one-out cross-validations of MNIRS-PLSR models indicated accurate predictions ( $R^2 > 0.90$ , negligible bias, ratio of performance to deviation  $> 3$ ) and fraction-specific functional group contributions to beta coefficients in the models. TOC and its fractions were predicted using the cross-validated models and soil spectra for 3109 reforested and agricultural soils. The reliability of predictions determined using *k*-nearest neighbour score distance indicated that  $>80\%$  of predictions were within the satisfactory inlier limit. The study demonstrated the utility of infrared spectroscopy (MNIRS-PLSR) to rapidly and economically determine TOC and its fractions and thereby accurately describe the effects of land use change such as reforestation on agricultural soils.

© 2017 Elsevier Ltd. All rights reserved.

## 1. Introduction

The soil organic carbon (SOC) pool is one of the largest terrestrial stores of carbon (C), containing about 1500 Gt C (Schlesinger,

\* Corresponding author.

E-mail addresses: [dineshbm@unimelb.edu.au](mailto:dineshbm@unimelb.edu.au), [madhavandinesh@gmail.com](mailto:madhavandinesh@gmail.com) (D.B. Madhavan).

1986). Consequently, even small changes in the amounts of soil C in response to land use, management or climate may have large effects on global C cycling and climate change. Reforestation is implemented around the world to sequester C and improve environmental conditions (e.g., water quality and habitat availability, Cunningham et al., 2015b). The total area of world's planted forest in 2010 was estimated to be 264 million ha, making up 6.6% of the world's forest area (FAO, 2010). In Australia, mixed-species environmental plantings are established on previous agricultural land for C sequestration and other environmental outcomes accounting up to 20% of the 1.14 million ha of reforestation between 1990 and 2012 (Paul et al., 2013). Studies have focused on improving measurement and modelling of biomass C following reforestation with environmental plantings (Paul et al., 2015; Perring et al., 2015), and measured associated changes in SOC (Cunningham et al., 2015a).

Conventional measurement of SOC as total organic C (TOC) using chemical oxidation (Walkley and Black, 1934) or dry combustion (Merry and Spouncer, 1988) is inadequate to explain changes in SOC in terms of soil physical, chemical and biological activity. Partitioning TOC into fractions that are related to active, intermediate or slow and passive or inert conceptual pools used in soil C turnover models (e.g., RothC, Jenkinson et al., 1992; CENTURY, Parton et al., 1987), can help elucidate their role in soil processes (Skjemstad et al., 2004). Such fractions may represent labile, humified and inert C with turnover times respectively of the order of annual (<3 year), decadal (20–50 year) and millennial (>1000 year, Jenkinson and Coleman, 1994). Several functional pools are known which are accessible by different fractionation methods. Physical fractions are such as aggregates, particle sizes and density fractions, chemical fractions are usually extracts (DOM, soil microbial biomass, organic matter soluble in alkali and acid, etc.) and also combinations of fractionation methods are used (von Lützwow et al., 2007).

Skjemstad et al. (2004) demonstrated that the RothC model could be initialised and changes in soil C stock simulated by replacing the conceptual stocks of resistant plant material (RPM), humus (HUM) and inert organic matter (IOM), respectively, with operationally measured particulate (POC), humus (HOC) and resistant (ROC) organic C. Subsequently, Janik et al. (2007) showed that the concentrations of POC, HOC and ROC in <2 mm sieved soil could be predicted from mid-infrared (MIR) spectra acquired from finely ground samples.

Diffuse reflectance mid-infrared spectroscopy (MIRS) is a rapid, non-destructive and low-cost technique, demonstrated to be suitable for routine analysis of a variety of soil properties (Soriano-Disla et al., 2014). The MIRS technique requires minimal sample preparation (i.e. air drying and fine grinding) and no use of hazardous chemicals. MIR spectra and corresponding analytical data in multivariate analyses such as partial least squares regression (PLSR) can be combined to develop prediction models for soil attributes. The predictive ability of MIRS-PLSR techniques for total, organic and inorganic C of soils has been well investigated and reported (Grinand et al., 2012; Madari et al., 2006; Madhavan et al., 2016). However, the use of MIRS-PLSR to predict the concentrations of fractions of TOC is limited (Bornemann et al., 2010; Janik et al., 2007; Zimmermann et al., 2007). MIRS-PLSR prediction models have been developed for total, organic and inorganic C, and TOC fractions (Baldock et al., 2013a), and these models were applied to predict the content of TOC fractions in subsequent agricultural soil C studies (Karunaratne et al., 2014; Rabbi et al., 2014). However, the applicability of such predictive models to soils under woody vegetation has not been investigated. Further, there is increasing interest in reforestation of agricultural lands to mitigate greenhouse gas emissions through sequestering C in woody biomass (Canadell and Raupach, 2008) and in soil (Lal, 2005). Thus, there is a need to develop accurate and efficient measurement techniques

and prediction models applicable to reforested land to understand and predict their potential to sequester C and mitigate greenhouse gas emissions.

An extensive study was conducted to investigate the changes in TOC and its fractions following reforestation with mixed-species environmental plantings at 117 sites from temperate, Mediterranean-type and tropical climatic regions of Australia, for the purpose of calibrating a soil C accounting model (FullCAM, Brack and Richards, 2002) developed from the RothC model (Paul et al., 2015), and to provide measurements and predictions of TOC fractions. Prediction models for TOC fractions have been reported in agricultural soils by Baldock et al., 2013a, but these models are unlikely to be accurate for reforested soils because of the difference in plant inputs, chemistry and decomposition rates between land uses, and thereby changes in TOC fractions (Del Galdo et al., 2003; Berthrong et al., 2012; Cunningham et al., 2015a). This warrants a need to develop infrared spectroscopic prediction models for TOC fractions that are suitable for soils under reforestation. This work presents the first attempt to develop prediction models for TOC fractions in a treed ecosystem whereas previous work has focused on agricultural soils (Baldock et al., 2013a). Our objectives were to measure soil TOC fractions (POC, HOC and ROC) in a representative set of reforested soils; develop robust infrared and PLSR prediction models for TOC and its fractions for reforested soils; and predict TOC and its fractions for both environmental planting and reference agricultural soils (i.e. pastures and cropping).

## 2. Methods

### 2.1. Soils

Soils were collected from 117 sites, each comprising a mixed-species environmental planting paired with an adjacent agricultural land use (Fig. 1). Details of site characteristics and sampling methods are detailed in England et al., 2016 and summarised here. The sites were across southern and eastern Australia (latitude 30.9

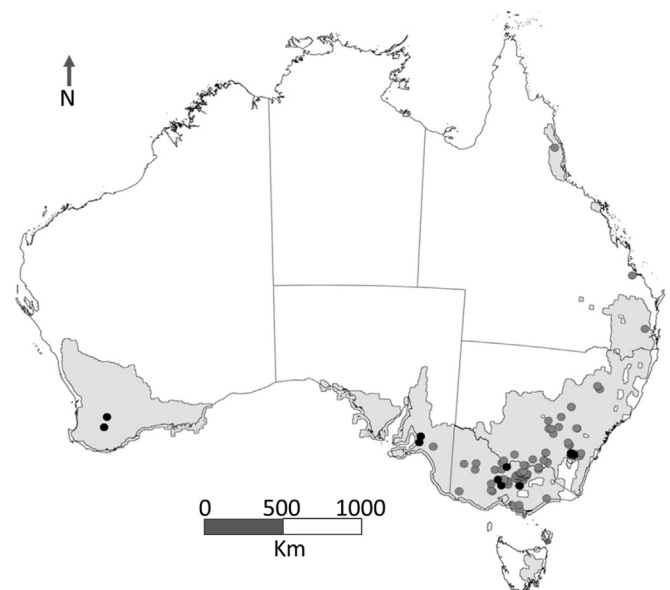


**Fig. 1.** Distribution of environmental planting sites and adjacent agricultural reference sites ( $n = 117$ , all circles). Soils from a subset of these plantings ( $n = 19$ , black circles) were physically fractionated. The shaded area represent the geographical regions of application of calibration for the environmental planting study area (after Paul et al., 2015).

to 38.7 °S, longitude 117.4 to 150.3 °E) and covered the range of rainfall zones where environmental plantings occur (380–1150 mm y<sup>-1</sup>). Generally the sites represented a range of planting age (mean age = 14 y, 95% of plantings aged between 1 and 28 y), surface soil texture (sandy loam, ≤ 20% clay to loam or clay, > 20% clay), productivity (above-ground biomass increment, 0.2–31.7 Mg DM ha<sup>-1</sup> y<sup>-1</sup>) and mixed-species plantings (e.g., *Acacia*, *Agathis*, *Araucaria*, *Castanospermum*, *Corymbia*, *Elaeocarpus*, *Eucalyptus*, *Flindersia*, *Khaya*, *Melaleuca*). Agricultural land use at the sites included grazing, cropping, and rotational cropping and grazing.

Soil samples were collected from each land-use at each site from formal plots or along transects, and to 30 cm depth variously in depth increments (cm): 0–5 & 5–30; 0–10 & 10–30; 0–5, 5–10 & 10–30; or 0–5, 5–10, 10–20 & 20–30. Individual samples for analysis (site × land use × depth, *n* = 3109) were generated by compositing (typically) 5 cores.

## 2.2. Soil processing and C analysis

Soil samples were air dried and manually sieved (≤ 2 mm) without crushing > 2 mm organic matter. The existing soils had been similarly air-dried and processed, and stored in air-tight containers at room temperature. Subsamples (approx. 20 g) of air dried ≤ 2 mm soil were finely ground in a vibratory 10 cm bowl steel puck mill (Rocklabs, Auckland, New Zealand) for 120 s (an additional 60 s for coarse textured soils, if required) to obtain a fine talc-like consistency, so as to ensure sub-sample homogeneity for chemical analysis and acquisition of consistent spectra across subsamples. TOC concentrations were determined on the finely ground ≤ 2 mm soil by Dumas high-temperature combustion (Rayment and Lyon, 2011) using a LECO CNS-2000 dry combustion analyser (LECO Corporation, St Joseph, MI, USA). Prior to TOC analyses, the finely ground ≤ 2 mm soil samples were tested for the presence of carbonates using 1 M HCl acid fizz test (Rayment and Lyon, 2011). Samples with carbonate were treated with 1 mL of 5–6% H<sub>2</sub>SO<sub>3</sub> at 100 °C until effervescence ceased (Nelson and Sommers, 1996) before drying and TOC analysis.

## 2.3. Acquisition of infrared spectra

Diffuse reflectance spectra (7800–450 cm<sup>-1</sup> at 4 cm<sup>-1</sup> resolution), which included the mid-infrared region and some of the near-infrared region, were acquired using a PerkinElmer Frontier FT-NIR/MIR Spectrometer (PerkinElmer Inc., Waltham, MA, USA) equipped with a KBr beam-splitter, a DTGS detector and AutoDiff automated diffuse reflectance accessory (Pike Technologies, Madison, WI, USA). Finely-ground soil samples (approx. 150–250 mg) were uniformly packed and levelled in 9 mm diameter stainless steel cups. Sixty cups and a background disc (silicon carbide) were loaded onto the Autodiff accessory and scanned. At the start of each scanning cycle, a background signal was collected from the silicon carbide disk (average of 240 scans) and subtracted from all sample spectra. For each soil sample, 64 co-added scans were acquired and averaged to obtain a representative reflectance spectrum (R). These reflectance spectra were converted to absorbance spectra (A) by the formula,  $A = \log(1/R)$  using PerkinElmer instrument control Spectrum 5.0.1 Software, which contained peaks corresponding to molecular vibrations of organic matter and minerals (absorbance units along Y axis) against specific wavenumbers (cm<sup>-1</sup> along X axis, Fig. 2a). The PerkinElmer specific spectral file format (.sp) was converted to the thermo galactic file format (.spc) using GRAMS/AI 9.1 (Thermo Fisher Scientific Inc., Waltham, MA USA). The absorbance spectra were later trimmed to 6000–450 cm<sup>-1</sup> for analyses.

## 2.4. Soil TOC fractionation

Soil samples from 19 environmental planting sites (0–5 and 5–10 cm depth, *n* = 38) across the geographical regions of the study area were selected for C fractionation. The soils were selected such that samples likely contained measureable quantities of the TOC fractions as indirectly indicated by TOC concentrations (>25 g kg<sup>-1</sup> in 0–5 cm and >15 g kg<sup>-1</sup> in 5–10 cm samples) and also to cover most of the observed range in TOC of all samples (0.7–93.1 g kg<sup>-1</sup>). The TOC fractionation methodology of Baldock et al. (2013b) was used to measure POC, HOC and ROC concentrations. Three 10 g replicates of ≤ 2 mm soil were dispersed using 45 mL of 5 g L<sup>-1</sup> sodium hexametaphosphate by shaking the tubes overnight. These samples were wet-sieved for 3 min through a 50 μm mesh using an automated vibratory sieve shaker (Analysette 3 PRO, FRITTSCH GmbH, Idar-Oberstein, Germany) with an amplitude of 2.5 mm at 20 s intervals and water flow rate of approx. 100 mL min<sup>-1</sup> to separate coarse (2000–50 μm) and fine fractions (≤ 50 μm). The fractions were lyophilized, coarse fractions were finely ground and analysed for total C concentration by Dumas high temperature combustion. Additional ≤ 2 mm soil was similarly fractionated where necessary to accumulate sufficient coarse and fine fraction material (equivalent of >20 mg of organic C) for measurement of ROC using solid-state <sup>13</sup>C NMR spectroscopy. Prior to NMR analysis, the coarse fractions were finely ground using a small pestle and mortar, and the fine fractions were treated with 2% HF (Skjemstad et al., 1994) to remove paramagnetic matter and concentrate organic C.

## 2.5. <sup>13</sup>C NMR spectroscopy

Spectra of <sup>13</sup>C NMR were acquired for the physically-fractionated coarse and fine fractions using a Bruker 200 Avance 200 MHz spectrometer (Bruker Corporation, Billerica, MA, USA), equipped with 4.7 T superconducting magnet operating at 50.33 MHz resonance (Baldock et al., 2013b). Samples (approx. 100–300 mg) of the coarse and fine fractions were packed in small zirconia rotors (7 mm diameter rotors fitted with Kel-F end caps) and spun at 5 KHz. For a few coarse fractions insufficient material was accumulated to completely fill the rotors, so 1 or 2 Kel-F inserts were used. All samples were subjected to a cross-polarisation (CP) <sup>13</sup>C NMR analysis in which 10,000 scans were acquired by applying a pulse of 3.2 μs, 195 W and 90°, with 1 ms contact time and 1 s recycle decay time. The length of the recycle delay time was confirmed to be more than 5 times the T<sub>1</sub>H value of the samples calculated using an inversion recovery pulse sequence. A variable spin lock experiment using various spin-lock times, 1 ms contact time and 1 s recycle delay determined sample specific T<sub>1</sub>ρH values. Glycine was used as an external intensity standard for comparing the observability of C in samples. Background signal correction was done by subtracting the signal intensity acquired for an empty rotor from the sample spectra. The NMR spectra were processed using the Bruker Topspin 3 software. Signal intensity found in the aryl (110–145 ppm) and O-aryl regions (145–165 ppm) of the NMR spectra (Fig. 2b) were used to calculate the proportions of lignin and ROC present in the coarse and fine fraction using the formula  $ROC = (\text{aryl C} - 1.77 * \text{O-aryl C}) / 0.45$  (Baldock et al., 2013b).

POC concentration was calculated by multiplying the TOC concentration of the coarse fraction by (1 – the proportion of ROC in the coarse fraction). Similarly HOC concentration was calculated by multiplying the TOC concentration of fine fraction by (1 – the proportion of ROC in the fine fraction). The recovery of TOC fractions was calculated as the percentage recovery of TOC using the formula,  $\text{Recovery\%} = [(POC + HOC + ROC) / TOC] * 100$ . The absolute deviation of recovery was calculated as the difference in the

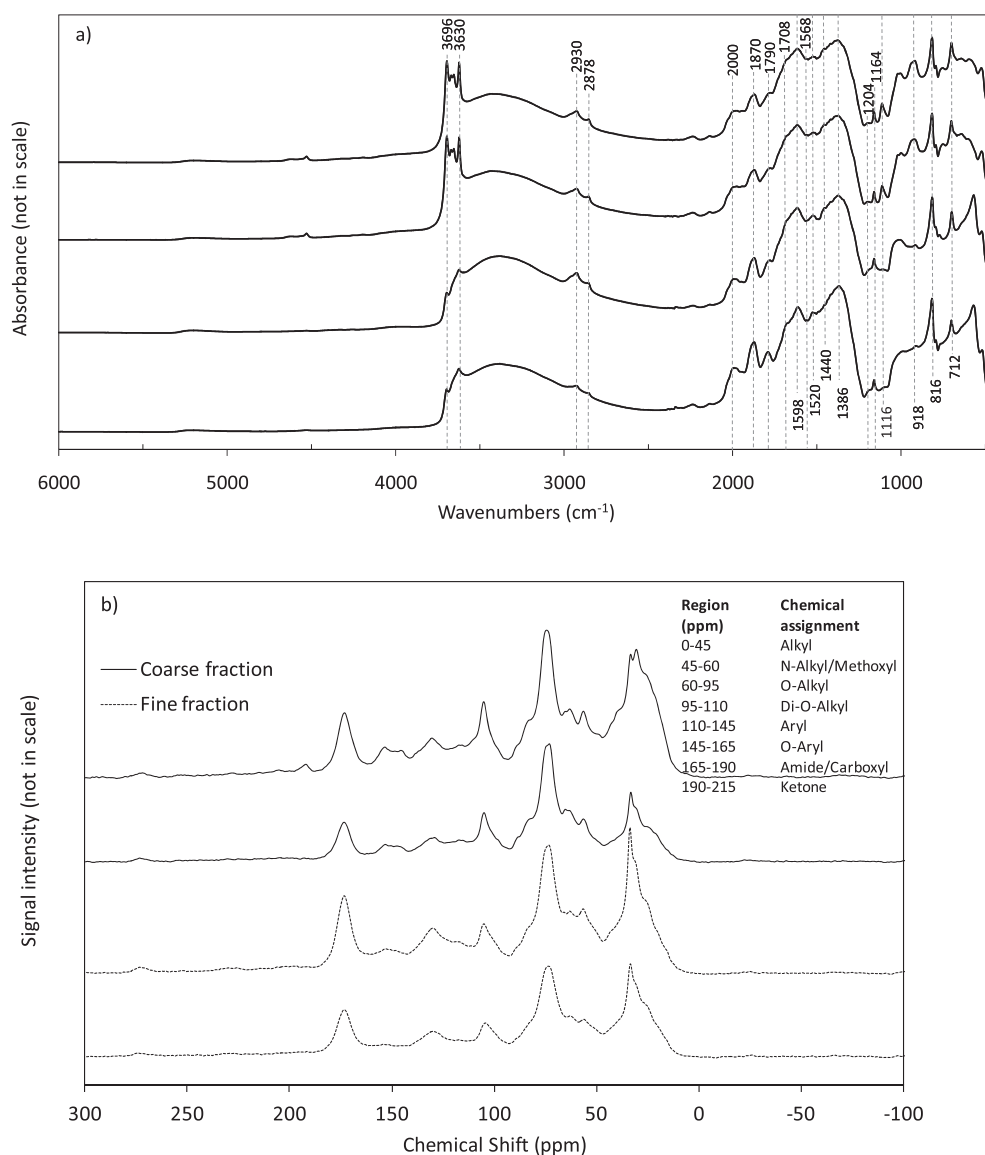


**Fig. 2.** Representative a) infrared spectra ( $6000\text{--}450\text{ cm}^{-1}$ ) acquired from finely-ground soils and b)  $^{13}\text{C}$  NMR spectra acquired from coarse ( $2000\text{--}50\text{ }\mu\text{m}$ ) and fine fractions ( $<50\text{ }\mu\text{m}$ ) of environmental planting soils.

measured concentrations between TOC and the sum of its fractions, and expressed in  $\text{g kg}^{-1}$ .

## 2.6. Infrared-PLSR calibrations and chemometrics

The PLSR models were developed as described by Haaland and Thomas (1988) using the infrared spectra and measured data from 38 environmental planting soils and 130 agricultural soil samples included from the Australian Soil Carbon Research Program (SCaRP, Baldock et al., 2013b). These prediction models were then used to predict TOC, POC, HOC and ROC in 3109 environmental plantings and agricultural soils.

Prior to multivariate analyses, the absorbance spectra were pre-processed using multiplicative scatter correction (Martens and Naes, 1989) and mean centring in Matlab R2013a (The MathWorks, Natick, MA, USA). Principal component analysis (PCA) and PLSR analysis were performed using PLS\_Toolbox 7.0 (Eigenvector Research Inc., Wenatchee, WA, USA). The mid-and near-infrared spectra (MNIRS) used for PCA and PLSR included the MIR spectral

region ( $4000\text{--}450\text{ cm}^{-1}$ ) corresponding to absorbance from fundamental bands of molecular vibrations, and a portion of the near-infrared (NIR) region ( $6000\text{--}4000\text{ cm}^{-1}$ ) containing overtones and combinations of fundamental bands but with less band specificity (Bellon-Maurel and McBratney, 2011). Baseline offset pre-processing of the MIR  $4000\text{--}450\text{ cm}^{-1}$  region produced inconsistent results by offsetting either in the middle or at the either end of spectral range. Pre-processing using the  $6000\text{--}450\text{ cm}^{-1}$  MNIRS spectral range produced more consistent offsetting around  $6000\text{--}5500\text{ cm}^{-1}$ . Therefore spectral information from both mid and near-infrared regions was used to develop the MNIRS-PLSR prediction models.

A square root transformation was used to normalise the distributions of TOC and its fraction concentrations and minimise non-linearity in the resultant PLSR prediction algorithm (Janik et al., 2007). A user-defined Matlab pre-processing function (*preprouser.m*) was used for the data transformation and back-transformation processes – *calibrate* and *apply* (applying square-root), and *undo* (squaring the model predictions). A PCA was

performed using the pre-processed soil spectra to be used to construct the PLSR prediction models to quantify their spectral variability. This PCA model was used to ascertain spectral homogeneity and detect potential outliers from the spectra acquired here for all reforested and agricultural soil samples in the present study (Viscarra Rossel et al., 2008).

The predictive abilities of the MNIRS-PLSR models were evaluated using a range of statistical parameters; coefficient of determination ( $R^2$ ), root mean square error (RMSE), bias, ratio of performance to deviation (RPD) and ratio of error range (RER) as commonly reported for assessing the quality of predicted soil attributes in spectroscopic studies (Bellon-Maurel and McBratney, 2011). These statistical analyses were made using PLS\_Toolbox and reported in back-transformed values.  $R^2$  indicates the model's fit, and root-mean-square error of calibration (RMSEC) and cross-validation (RMSECV) are measures of standard deviation of the residuals in calibration and in cross-validation respectively. Bias is the mean value of the difference between predicted and measured values. RPD is the ratio of standard deviation of measured values to standard error of prediction (Bellon-Maurel and McBratney, 2011). The RER is the ratio of the range of the predicted data (maximum – minimum) to RMSE. Generally, strong prediction models are expected to contain high values for  $R^2$ , minimum values for RMSE and RPD > 2 (Grinand et al., 2012), and RER > 10 (Williams and Sobering, 1996). The number of principal components (PCs) in a given PCA model, and factors or latent variables (LV) contributing to each PLSR model was restricted when the following PC or LV did not reduce the RMSE of calibration by more than 1%. The robustness of the MNIRS-PLSR models were also investigated by examining the variations in beta coefficients and Variable Importance in Projection (VIP) scores (Chong and Jun, 2005), which reveal the infrared bands and specific functional groups that contributed the most to the prediction models of TOC fractions, and helped to distinguish fraction-specific organic C composition at the functional-group level.

### 2.7. Prediction assessments

The reliability of predictions from MNIRS-PLSR models were evaluated by using  $k$ -nearest neighbour (KNN) score distances (Sharaf et al., 1986), calculated in PLS\_Toolbox software. The KNN score distance is the distance to the nearest neighbour (shortest distance) in the three-dimensional score space of the samples (Ripley, 1996), and scalar value ' $k$ ' indicates the number of neighbours to which distance should be calculated and averaged over. The scalar was set to  $k = 1$  as described in ASTM D6122-06 Standard Practice for Validation of the Performance of Multivariate Process Infrared Spectrophotometers, (ASTM International, West Conshohocken, PA, USA). The scalar setting was performed in Matlab using the command: `setplsprep ('plotscores','knnscoredistance',1)`. The maximum KNN score distance observed for samples in the calibration is called the inlier limit. Prediction samples outside the inlier limit suggest that they fall within a sparsely populated region of the calibration space (ASTM International, 2006). Classification and neighbour selection studies generally use a Mahalanobis

distance of 3 or more to determine non-members or spectral outliers (Gogé et al., 2012). As KNN score distance and Mahalanobis distance are highly correlated (Wise et al., 2006), predicted samples with higher KNN score distance, i.e. more than 3 times of inlier limit were considered as having unreliable predictions. Hotelling's  $T^2$  represents the measure of the variation in each sample within the model and indicates how far each sample is from the center of the model. Hotelling  $T^2$  contribution was used to reveal how individual variables (spectral wavenumbers) contributed to unusual variation in predicted outlier samples as determined by inlier test (Kourti, 2005).

## 3. Results and discussion

### 3.1. Soil TOC fractions from environmental plantings

The concentration ranges of TOC and its fractions in the environmental plantings soils used for fractionation are provided in Table 1. The recovery of TOC after fractionation was similar to that obtained by Baldock et al. (2013b) and ranged between 87 and 112%, with a mean recovery of 94%, and a standard deviation of 5.6%. The absolute deviation of recovery of TOC fractions indicated that for >90% of the samples, TOC recovery was within  $\pm 2 \text{ g kg}^{-1} \text{ }^\circ\text{C}$  with the variation in absolute recovery increasing with increasing TOC concentration. When expressed as percentage of TOC, POC ranged between 8.1% and 54.0% (mean  $\pm$  SD =  $25.8 \pm 12.5\%$ ), with 35.5% and 16.9% in the 0–5 cm and 5–10 cm layers, respectively. HOC ranged between 30.3 and 72.5% (mean  $\pm$  SD =  $52.1 \pm 10.8\%$ ), and ROC ranged between 15.5 and 31.7% (mean  $\pm$  SD =  $20.4 \pm 3.44\%$ ). By comparison, in agricultural soils representing the range of soil types and climate across the productive land in Australia (organic C ranging from 10.0 to 91.0  $\text{g kg}^{-1}$  soil), the mean proportions were  $19.2 \pm 12.3\%$  for POC,  $56.1 \pm 14.5\%$  for HOC and  $26.2 \pm 9.6\%$  for ROC in TOC (Baldock et al., 2013b).

The concentrations of TOC fractions were correlated with soil TOC concentration ( $R^2 = 0.83$  for POC;  $R^2 = 0.73$  for HOC;  $R^2 = 0.84$  for ROC,  $P < 0.05$ ). Relationship slopes of 0.55, 0.30 and 0.16 for POC, HOC and ROC, respectively, were higher for POC, lower for HOC and similar for ROC in 0–10 cm environmental plantings soils when compared to those obtained by Baldock et al. (2013b) for agricultural soils having similar TOC concentrations (1.20–95.0  $\text{g kg}^{-1}$ ). These results suggest that on average soils under environmental plantings contain more POC and less HOC compared to agricultural soils.

### 3.2. PCA of samples

The first three PCs of the PCA of spectra acquired for the environmental plantings and the agricultural soils explained 94% of the model's variation. The distribution of PC scores indicated that the spectra from environmental planting soils differed from those of the agriculture soils, largely due to differences in the PC2 and PC3 scores (Fig. 3a). The PC1 loading spectra which accounted for 69.7% of spectral variance showed absorbance intensity mostly from soil mineral components (Fig. 3b). In contrast, PC2 (19% of spectral

**Table 1**  
Concentration range, mean and standard error (SE) of soil (0–5, 5–10 cm) TOC and TOC fractions in 19 environmental plantings sites.

Depth (cm)	(g kg <sup>-1</sup> soil)											
	TOC			POC			HOC			ROC		
	Range	Mean	SE	Range	Mean	SE	Range	Mean	SE	Range	Mean	SE
0–5	26.2–59.9	40.9	2.5	5.6–29.5	14.8	1.8	11.8–25.1	17.2	0.9	4.8–10.7	7.8	0.4
5–10	15.1–29.8	20.4	1.0	1.4–6.6	3.0	0.3	8.0–19.2	11.1	0.8	2.9–6.9	4.4	0.3

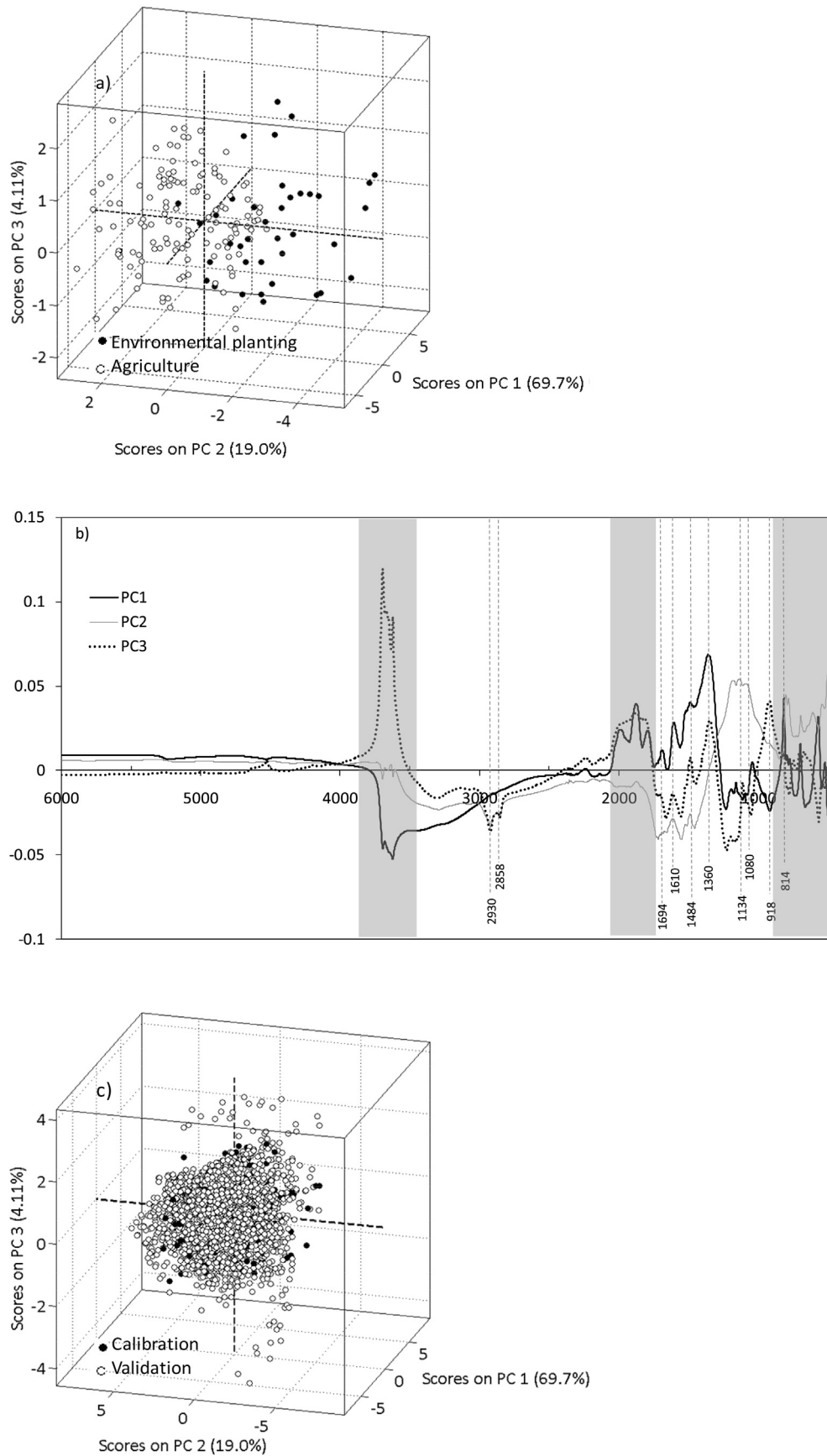


**Fig. 3.** Principal components analyses of near- and mid-infrared spectra (6000–450 cm<sup>-1</sup>) for soils: (a) 3D scores plot for fractionated soils used to develop PLSR prediction models (38 environmental planting soils, present study; 130 agricultural soils, Baldock et al., 2013a); (b) Principal component (PC) loadings against wavenumbers (cm<sup>-1</sup>) for the fractionated soils showing major organic bands in broken lines and regions dominated by mineral bands in grey; and (c) 3D scores plot for all soils (calibration, n = 168, predicted, n = 3109). For the 3D scores plots, values in parentheses are percentage of spectral variance explained by each component.

**Table 2**  
Major peaks in the soil infrared spectra and loadings and their functional group assignments.

Wavenumber (cm <sup>-1</sup> )	Functional group	Vibration	References
3696, 3630	Kaolinite, montmorillonite and illite	O–H stretching	Viscarra Rossel et al., 2008
2930, 2878	Alkyl	C–H stretching	Janik et al., 2007
2000, 1870, 1784	Quartz	Si–O stretching	Nguyen et al., 1991
1740 to 1710	Carboxylic acid	–COOH stretching	Janik et al., 2007
1666	Carbonyls of amide-I	C=O stretching	Janik et al., 2007; Bornemann et al., 2010
1610 to 1590	Aromatic; carboxylates	C=C stretching; COO– symmetric stretching	Haberhauer et al., 1998
1568	Amide II	C=N stretching	Janik et al., 2007; Ludwig et al., 2008
1520 to 1510	Aromatic	C=C stretching	Haberhauer et al., 1998
1484 to 1440	Alkyl	C–H deformation	Janik et al., 2007; Viscarra Rossel et al., 2008
1380 to 1360	Phenol	C–O stretching, O–H deformation	Bornemann et al., 2010
1280–1200	Carboxylic acid and phenol; ester	–COOH and C–O stretching; O–H deformation	Bornemann et al., 2010
1200 to 950	Carbohydrates; alumina-silicate of clay minerals	C–O, –COH and C–O–C stretching; Al–O–Si, Si–O–Si and Al–O–Al lattice vibrations	Ludwig et al., 2008; Bornemann et al., 2010;
915, 816, 712,	Aromatics; clay minerals and quartz	C–H deformation; O–H deformation, Si–O stretching	Nguyen et al., 1991; Haberhauer et al., 1998

variance) and PC3 (4.1% of spectral variance) showed distinct features associated with lignin and polysaccharide molecules with signals from aliphatic C–H stretch at 2930, 2858 and 1484 cm<sup>-1</sup>, carboxylic acid –COOH stretch at 1710 cm<sup>-1</sup> and C–O stretch at 1224 cm<sup>-1</sup>, amide I C=O stretch at 1666 cm<sup>-1</sup>, and amide II C–N stretch and potentially aromatic C=C stretch at 1556 cm<sup>-1</sup> that differentiated the environmental planting soils from the agricultural soils (Table 2). Projection of PC1, PC2 and PC3 scores for all other soil samples collected in this project ( $n = 3109$ ) onto the 3D scores plot of the calibration samples (Fig. 3c) showed a large cluster of samples within a three dimensional space defined by the calibration samples, indicating the similarity of spectra in both sets. A few samples were distributed away from the main cluster along the negative axis of PC1 and PC2 scores. These 16 samples (upper 5%) originated from a site having relatively high TOC concentration (>150 g kg<sup>-1</sup> soil) and had regular spectra with spectral features similar to other spectra collected here, and were therefore retained and included in subsequent analyses.

### 3.3. MNIRS-PLSR models and cross-validations

The predictive ability of MNIRS-PLSR models was tested using

**Table 3**  
Statistics for MNIRS-PLSR calibrations (Cal) and leave-one-out cross-validations (CV) for TOC, POC, HOC and ROC. Samples ( $n$ ) included 38 environmental planting soils and 53–130 agricultural soils. Spectra (6000–450 cm<sup>-1</sup>) were multiplicative scatter corrected and mean centered prior to PLSR analysis. RMSE = Root mean square error, RPD = Ratio of performance to deviation and RER = Ratio of error range.

	TOC		POC		HOC		ROC	
	Cal	CV	Cal	CV	Cal	CV	Cal	CV
$n$	153	91	154	168	154	168	154	168
Minimum (g kg <sup>-1</sup> soil)	2.1	1.3	1.4	0.4	1.4	0.4	1.4	0.4
Maximum (g kg <sup>-1</sup> soil)	90.2	30.5	34.5	17.8	34.5	17.8	34.5	17.8
Mean (g kg <sup>-1</sup> soil)	23.5	10.0	11.4	5.63	11.4	5.63	11.4	5.63
Standard deviation	14.9	5.7	6.9	3.3	6.9	3.3	6.9	3.3
Latent variables	6	7	6	7	6	7	6	7
Slope	0.95	0.93	0.88	0.86	0.91	0.89	0.91	0.89
Intercept	1.17	1.55	0.96	1.38	0.95	1.10	0.46	0.58
$R^2$	0.97	0.96	0.92	0.88	0.93	0.92	0.92	0.90
RMSE	2.68	3.04	1.67	1.97	1.75	1.97	0.93	1.05
Bias	-0.08	-0.07	-0.07	-0.05	-0.07	-0.06	-0.04	-0.04
RPD	5.59	4.84	3.42	2.89	3.90	3.47	3.57	3.15
RER	32.8	28.4	17.4	14.8	18.9	17.3	18.7	16.6

leave-one-out cross-validation (Table 3). Previous studies have used 10 to 13 latent variables for TOC fraction models (e.g., Janik et al., 2007) but the PLSR models developed here required only 6 or 7 latent variables to explain the maximum variation in spectra and the measured analytical data (TOC and its fractions). Scatter plots of measured and predicted data showed strong linear relationships for all prediction models ( $R^2 > 0.92$ ). The PLSR prediction model for TOC in the range of 0.20–100 g kg<sup>-1</sup> resulted in an RMSE of 2.68, negligible bias and an RPD of 5.59. Similarly, the PLSR models developed for TOC fractions showed RMSE values of approximately 5% of the data range used in their derivation, negligible bias and RPD values > 3.42.

The results obtained from cross-validation for TOC and its fractions were similar to calibration. Cross-validation of TOC resulted in excellent prediction ( $R^2 = 0.95$ , bias = -0.07, RMSE = 3.04 and RPD = 4.84), consistent with other reports for soils (Janik et al., 2007; Viscarra Rossel et al., 2008). Similar predictions ( $R^2 = 0.95$ ) have been found for TOC in Mediterranean soils with a comparable TOC range (5–150 g kg<sup>-1</sup>, D'Acqui et al., 2010). Janik et al. (2007) reported POC calibrations under native vegetation of Australia with  $R^2 = 0.71$  (range 0.20–16.8 g kg<sup>-1</sup>) and suggested that the variations in the chemistry of plant inputs may influence the development of accurate generalised prediction models. Here, POC predictions within the range of 0.20–16.8 g kg<sup>-1</sup> were relatively stronger for both calibration ( $R^2 = 0.88$ ) and cross-validation ( $R^2 = 0.86$ ). This is consistent with the results reported by (Baldock et al., 2013a). The RPD values for TOC and its fractions derived in this study were all >3. Although RPD in cross-validation results were slightly lower than the prediction model, all values were >2.89, which indicated excellent predictive ability of models, as suggested by Grinand et al. (2012).

### 3.4. Functional group analysis of models

Beta coefficients of the derived PLSR prediction models plotted against the wavenumbers illustrate the major functional groups and relative magnitude of their contributions to each prediction model (Fig. 4). For TOC, the dominant organic peaks were aliphatic C–H stretch (2930 and 2878 cm<sup>-1</sup>), carboxylic –COOH stretch (1708 cm<sup>-1</sup>), carbonyls and amide I and II C=O or C=N stretch (1666 and 1568 cm<sup>-1</sup>), aliphatic C–H deformations (1440 cm<sup>-1</sup>), carboxylic acid (1204 cm<sup>-1</sup>) and carbohydrates C–O or –COH stretch (1080 cm<sup>-1</sup>). Janik et al. (2007) reported similar spectral

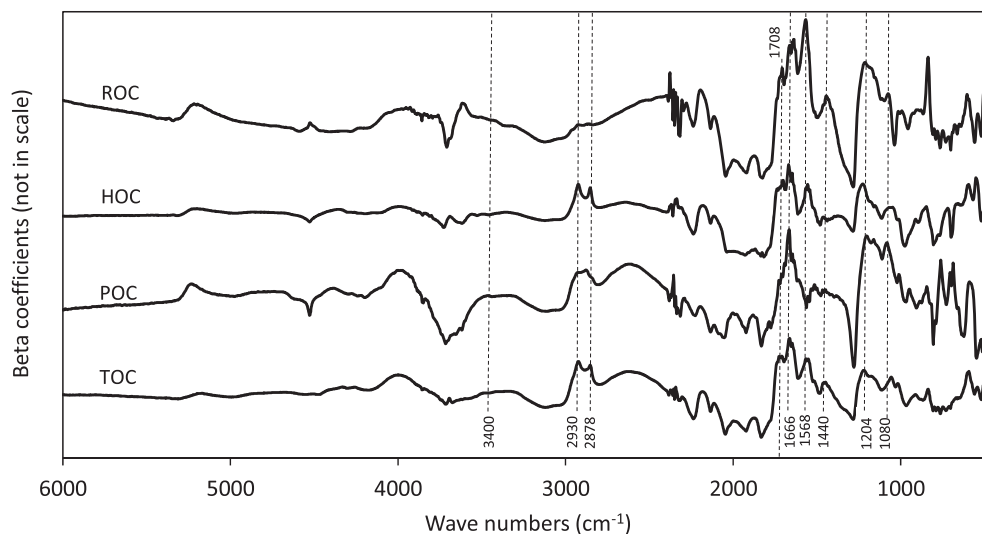


Fig. 4. Beta coefficients from MNIRS-PLSR prediction models for TOC, POC, HOC and ROC showing functional group-specific peaks (dotted lines).

features for their TOC model in average beta coefficients. For POC, in addition to some features noted for TOC, strong peaks of amides (C=O stretch,  $1666\text{ cm}^{-1}$ ), polysaccharides and silicate absorbance (C–O and Si–O stretch,  $1200\text{--}1080\text{ cm}^{-1}$ ), and distinct peaks of aromatic skeletal C=C stretching vibrations ( $1520\text{ cm}^{-1}$ ) and aromatic C=C stretch ( $1598\text{ cm}^{-1}$ ) were evident, indicating functional groups from proteins and carbohydrates. The correlation of beta coefficients derived for TOC with those derived for POC and ROC ( $R^2 \sim 0.50$ ) showed significant scatter indicating differences in spectral features and magnitudes used to predict these components and suggested a degree of independence between the derived prediction models (Fig. S1). The beta coefficients of TOC and HOC were highly correlated ( $R^2 = 0.75$ ) as reported by Baldock et al. (2013a). However, the beta coefficient for HOC had subtle differences in magnitudes and shifts in peaks, with higher contributions from carboxylic acids ( $1740$  and  $1240\text{ cm}^{-1}$ ). For ROC, most of the regions differed from that of other fractions, such as absence of aliphatic C–H ( $3000\text{--}2800\text{ cm}^{-1}$ ) and phenols ( $\sim 1380\text{ cm}^{-1}$ ) ascribed to lignin, and increased intensities from aromatic C=C ( $1570\text{ cm}^{-1}$ ), –COOH ( $1708\text{ cm}^{-1}$ ) and C–O ( $1228\text{ cm}^{-1}$ ) from carboxylic acid, aromatic C–H stretch ( $840\text{ cm}^{-1}$ ) and kaolinite ( $3626\text{ cm}^{-1}$ ).

Peaks with VIP scores  $>1$  significantly contributed to the model, while wavenumber  $<1$  was less important (Chong and Jun, 2005). Here, VIP scores in the MNIRS-PLSR models included C–H ( $2930$  and  $2878\text{ cm}^{-1}$ ) and C=O ( $1666\text{ cm}^{-1}$ ) for TOC and all fractions (VIP score  $> 2.8$ ); carboxylic acid C–O stretch, O–H deformation, ester and phenol C–O ( $1280\text{--}1200\text{ cm}^{-1}$ ), carbohydrate ( $1160\text{--}1080\text{ cm}^{-1}$ ), and aromatic and mineral absorbances ( $<1000\text{ cm}^{-1}$ ) for POC (VIP score  $> 4$ ); and aromatic C=C absorbance ( $1568\text{ cm}^{-1}$ ) for ROC (VIP score = 3.85) (Fig. S2). These functional groups were similar to the inferences from beta coefficients specific to TOC and its fractions in their models.

### 3.5. Predictions of TOC, POC, HOC and ROC contents

Using the leave-one-out cross-validated MNIRS-PLSR prediction models, TOC and its fractions were predicted in 3109 soils from environmental plantings and reference agricultural lands. The KNN score distance for the predicted samples indicated that  $>75\%$  of the predictions fell within the inlier limit (TOC-88.2%, POC-84.8%, HOC-75.8% and ROC-84.5%), while the remaining samples were within

the satisfactory limits of  $3 \times$  inlier limit, except for a few samples (TOC = 4, POC = 3, HOC = 6, ROC = 5, Fig. S3). KNN score distance is higher for samples that fall in lower-populated regions of score space (Wise et al., 2006). Predicted samples with high C content that were scattered in the PCA were within the inlier limits, so their inclusion was reasonable.

Hotelling  $T^2$  described  $>96\%$  of sample distribution within all models, hence it was useful in identifying the spectral regions contributing to unusual variations in the samples containing highest KNN scores (Wise et al., 2006). Hotelling  $T^2$  contributions for outlier samples showed increased intensities from mineral bands at  $4000\text{--}3500$  and  $1080\text{--}450\text{ cm}^{-1}$  and inorganic C and quartz bands at  $2200\text{--}1800\text{ cm}^{-1}$  (Fig. S4). These results were consistent with dominant site characteristics, i.e. a site with sandy texture from Western Australia and another site containing inorganic C from Victoria.

### 3.6. Application of the models

An example of the application of the MNIRS-PLSR models indicates that concentrations of POC and ROC in 0–5 cm soil ( $n = 79$ ) were on-average greater under environmental plantings ( $12.2$  and  $7.9\text{ g kg}^{-1}$  respectively) than under agricultural land-use ( $10.9$  and  $7.0\text{ g kg}^{-1}$  respectively), but that there is much variability from site to site (Fig. S5). A more detailed analysis of differences in TOC and in MNIRS-PLSR predicted values of TOC fractions between environmental planting and agriculture soils was reported in England et al. (2016).

The site to site variability demands that at least for landscape level studies and C accounting rapid analytical methodologies such as developed here are essential. While the models developed here were satisfactorily cross-validated, they remain specific calibrations for the environments (climatic, edaphic) and vegetation from which the soils were sampled, notwithstanding that the samples were from a range of environments across southern and eastern Australia. We might expect that marked differences in climate (e.g., arid zones), in soil parent material and soil mineralogy, in properties of plant organic matter added to the soil, and in management practices (e.g., tillage, prescribed burning) might challenge the model calibrations. While models for TOC seem relatively robust, those for the POC and HOC at least are less so and likely will always require very specific local based calibrations.

#### 4. Conclusions

We developed accurate MNIRS-PLSR predictive models for TOC and TOC fractions under reforested environments for application on a national/continental scale. The study demonstrated the potential of MNIRS-PLSR technique to rapidly and cost-effectively predict soil TOC and its fractions and thereby assess the magnitude of changes following reforestation. The technique has the potential for use in regional to global carbon accounting in reforested ecosystems. There is a need to build a broad database of soil TOC and TOC fractions for a wider range of climate, soils, vegetation and management to enable local to general calibration and validation of models.

#### Acknowledgements

The study was funded by the Australian Government's Filling the Research Gap program. TRC is supported by an Australian Research Council (ARC) Future Fellowship (FT120100463). MPP was partially supported through an ARC Laureate Fellowship to R. Hobbs. We acknowledge M. Bullock, T. Fairman, R. Greene, P. Holliday, R. Law, J. McGowan, T. Morald, T. Murshed, A. Schapel, G. Szegedy and A. Wherrett for provision of soil samples and field and laboratory support.

#### Appendix A. Supplementary data

Supplementary data related to this article can be found at <http://dx.doi.org/10.1016/j.jenvman.2017.02.013>.

#### References

- ASTM International, 2006. ASTM D6122-06, Standard Practice for Validation of the Performance of Multivariate Process Infrared Spectrophotometers. ASTM International, West Conshohocken, PA, USA.
- Baldock, J.A., Hawke, B., Sanderman, J., Macdonald, L.M., 2013a. Predicting contents of carbon and its component fractions in Australian soils from diffuse reflectance mid-infrared spectra. *Soil Res.* 51, 577–595.
- Baldock, J.A., Sanderman, J., Macdonald, L.M., Puccini, A., Hawke, B., Szarvas, S., McGowan, J., 2013b. Quantifying the allocation of soil organic carbon to biologically significant fractions. *Soil Res.* 51, 561–576.
- Bellon-Maurel, V., McBratney, A., 2011. Near-infrared (NIR) and mid-infrared (MIR) spectroscopic techniques for assessing the amount of carbon stock in soils – critical review and research perspectives. *Soil Biol. Biochem.* 43, 1398–1410.
- Berthrong, S.T., Piñeiro, G., Jobbágy, E.G., Jackson, R.B., 2012. Soil C and N changes with afforestation of grasslands across gradients of precipitation and plantation age. *Ecol. Appl.* 22, 76–86.
- Bornemann, L., Welp, G., Amelung, W., 2010. Particulate organic matter at the field scale: rapid acquisition using mid-infrared spectroscopy. *Soil Sci. Soc. Am. J.* 74, 1147–1156.
- Brack, C.L., Richards, G.P., 2002. Carbon accounting model for forests in Australia. *Environ. Pollut.* 116 (Suppl. 1), S187–S194.
- Canadell, J.G., Raupach, M.R., 2008. Managing forests for climate change mitigation. *Science* 320, 1456–1457.
- Chong, I.G., Jun, C.H., 2005. Performance of some variable selection methods when multicollinearity is present. *Chemom. Intell. Lab.* 78, 103–112.
- Cunningham, S.C., Cavagnaro, T.R., Mac Nally, R., Paul, K.I., Baker, P.J., Beringer, J., Thomson, J.R., Thompson, R.M., 2015a. Reforestation with native mixed-species plantings in a temperate continental climate effectively sequesters and stabilizes carbon within decades. *Glob. Change Biol.* 21, 1552–1566.
- Cunningham, S.C., Mac Nally, R., Baker, P.J., Cavagnaro, T.R., Beringer, J., Thomson, J.R., Thompson, R.M., 2015b. Balancing the environmental benefits of reforestation in agricultural regions. *Perspect. Plant Ecol. Evol. Syst.* 17, 301–317.
- D'Acqui, L.P., Pucci, A., Janik, L.J., 2010. Soil properties prediction of western Mediterranean islands with similar climatic environments by means of mid-infrared diffuse reflectance spectroscopy. *Eur. J. Soil Sci.* 61, 865–876.
- Del Galdo, I., Six, J., Peressotti, A., Francesca Cotrufo, M., 2003. Assessing the impact of land-use change on soil C sequestration in agricultural soils by means of organic matter fractionation and stable C isotopes. *Glob. Change Biol.* 9, 1204–1213.
- England, J.R., Paul, K.I., Cunningham, S.C., Madhavan, D.B., Baker, T.G., Read, Z., Wilson, B.R., Cavagnaro, T.R., Lewis, T., Perring, M.P., Herrmann, T., Polglase, P.J., 2016. Previous land use and climate influence differences in soil organic carbon following reforestation of agricultural land with mixed-species plantings. *Agric. Ecosyst. Environ.* 227, 61–72.
- FAO, 2010. Global Forest Resources Assessment 2010. Main Report, Rome.
- Gogé, F., Joffre, R., Jolivet, C., Ross, I., Ranjard, L., 2012. Optimization criteria in sample selection step of local regression for quantitative analysis of large soil NIRS database. *Chemom. Intell. Lab.* 110, 168–176.
- Grinand, C., Barthes, B.G., Brunet, D., Kouakoua, E., Arrouays, D., Jolivet, C., Caria, G., Bernoux, M., 2012. Prediction of soil organic and inorganic carbon contents at a national scale (France) using mid-infrared reflectance spectroscopy (MIRS). *Eur. J. Soil Sci.* 63, 141–151.
- Haaland, D.M., Thomas, E.V., 1988. Partial least-squares methods for spectral analyses. 1. Relation to other quantitative calibration methods and the extraction of qualitative information. *Anal. Chem.* 60, 1193–1202.
- Haberhauer, G., Rafferty, B., Strebl, F., Gerzabek, M.H., 1998. Comparison of the composition of forest soil litter derived from three different sites at various decomposition stages using FTIR spectroscopy. *Geoderma* 83, 331–342.
- Janik, L.J., Skjemstad, J.O., Shepherd, K.D., Spouncer, L.R., 2007. The prediction of soil carbon fractions using mid-infrared-partial least square analysis. *Aust. J. Soil Res.* 45, 73–81.
- Jenkinson, D.S., Coleman, K., 1994. Calculating the annual input of organic matter to soil from measurements of total organic matter and radiocarbon. *Eur. J. Soil Sci.* 45, 167–174.
- Jenkinson, D.S., Harkness, D.D., Vance, E.D., Adams, D.E., Harrison, A.F., 1992. Calculating net primary production and annual input of organic matter to soil from the amount and radiocarbon content of soil organic matter. *Soil Biol. Biochem.* 24, 295–308.
- Karunaratne, S.B., Bishop, T.F.A., Baldock, J.A., Odeh, I.O.A., 2014. Catchment scale mapping of measureable soil organic carbon fractions. *Geoderma* 219–220, 14–23.
- Kourti, T., 2005. Application of latent variable methods to process control and multivariate statistical process control in industry. *Int. J. Adapt. Control Signal Process* 19, 213–246.
- Lal, R., 2005. Forest soils and carbon sequestration. *For. Ecol. Manage* 220, 242–258.
- Ludwig, B., Nitschke, R., Terhoeven-Urselmans, T., Michel, K., Flessa, H., 2008. Use of mid-infrared spectroscopy in the diffuse-reflectance mode for the prediction of the composition of organic matter in soil and litter. *J. Plant Nutr. Soil Sci. Zeitschrift Fur Pflanzenernahrung Und Bodenkd.* 171, 384–391.
- Madari, B.E., Reeves Iii, J.B., Machado, P.L.O.A., Guimaraes, C.M., Torres, E., McCarty, G.W., 2006. Mid- and near-infrared spectroscopic assessment of soil compositional parameters and structural indices in two Ferralsols. *Geoderma* 136, 245–259.
- Madhavan, D.B., Kitching, M., Mendham, D.S., Weston, C.J., Baker, T.G., 2016. Mid-infrared spectroscopy for rapid assessment of soil properties after land use change from pastures to Eucalyptus globulus plantations. *J. Environ. Manage* 175, 67–75.
- Martens, H., Naes, T., 1989. *Multivariate Calibration*. John Wiley & Sons, New York, USA.
- Merry, R.H., Spouncer, L.R., 1988. The measurement of carbon in soils using a microprocessor-controlled resistance furnace. *Commun. Soil Sci. Plant Anal.* 19, 707–720.
- Nelson, D.W., Sommers, L.E., 1996. Total carbon, organic carbon, and organic matter. In: Sparks, D.L. (Ed.), *Methods of Soil Analysis. Part 3-Chemical Methods*. Soil Science Society of America Inc. and American Society of Agronomy Inc., Madison, Wisconsin, USA, pp. 961–1010.
- Nguyen, T.T., Janik, L.J., Raupach, M., 1991. Diffuse reflectance infrared fourier-transform (drift) spectroscopy in soil studies. *Aust. J. Soil Res.* 29, 49–67.
- Parton, W.J., Schimel, D.S., Cole, C.V., Ojima, D.S., 1987. Analysis of factors controlling soil organic matter levels in great plains grasslands. *Soil Sci. Soc. Am. J.* 51, 1173–1179.
- Paul, K.I., Reeson, A., Polglase, P., Crossman, N., Freudenberger, D., Hawkins, C., 2013. Economic and employment implications of a carbon market for integrated farm forestry and biodiverse environmental plantings. *Land Use Policy* 30, 496–506.
- Paul, K.I., Roxburgh, S.H., England, J.R., de Ligt, R., Larmour, J.S., Brooksbank, K., Murphy, S., Ritson, P., Hobbs, T., Lewis, T., Preece, N.D., Cunningham, S.C., Read, Z., Clifford, D., John Raison, R., 2015. Improved models for estimating temporal changes in carbon sequestration in above-ground biomass of mixed-species environmental plantings. *For. Ecol. Manage* 338, 208–218.
- Perring, M.P., Jonson, J., Freudenberger, D., Campbell, R., Rooney, M., Hobbs, R.J., Standish, R.J., 2015. Soil-vegetation type, stem density and species richness influence biomass of restored woodland in south-western Australia. *For. Ecol. Manage* 344, 53–62.
- Rabbi, S.M.F., Tighe, M., Cowie, A., Wilson, B.R., Schwenke, G., McLeod, M., Badger, W., Baldock, J., 2014. The relationships between land uses, soil management practices, and soil carbon fractions in South Eastern Australia. *Agric. Ecosyst. Environ.* 197, 41–52.
- Rayment, G.E., Lyon, D.J., 2011. *Soil Chemical Methods - Australasia*. CSIRO Publishing, Melbourne, Australia.
- Ripley, B.D., 1996. *Pattern Recognition and Neural Networks*. Cambridge University Press, Cambridge, UK.
- Schlesinger, W.H., 1986. Changes in soil carbon storage and associated properties with disturbance and recovery. In: Trabalka, J.R., Reichle, D.E. (Eds.), *The Changing Carbon Cycle*. Springer, New York, pp. 194–220.
- Sharaf, M.A., Illman, D.L., Kowalski, B.R., 1986. *Chemometrics*. John Wiley & Sons, New York.
- Skjemstad, J., Clarke, P., Taylor, J., Oades, J., Newman, R., 1994. The removal of magnetic materials from surface soils - a solid state <sup>13</sup>C CP/MAS NMR study. *Soil Res.* 32, 1215–1229.

- Skjemstad, J.O., Spouncer, L.R., Cowie, B., Swift, R.S., 2004. Calibration of the Rothamsted organic carbon turnover model (RothC ver. 26.3), using measurable soil organic carbon pools. *Aust. J. Soil Res.* 42, 79–88.
- Soriano-Disla, J.M., Janik, L.J., Viscarra Rossel, R.A., MacDonald, L.M., McLaughlin, M.J., 2014. The performance of visible, near-, and mid-infrared reflectance spectroscopy for prediction of soil physical, chemical, and biological properties. *Appl. Spectrosc. Rev.* 49, 139–186.
- Viscarra Rossel, R.A., Jeon, Y.S., Odeh, I.O.A., McBratney, A.B., 2008. Using a legacy soil sample to develop a mid-IR spectral library. *Aust. J. Soil Res.* 46, 1–16.
- von Lütow, M., Kögel-Knabner, I., Ekschmitt, K., Flessa, H., Guggenberger, G., Matzner, E., Marschner, B., 2007. SOM fractionation methods: relevance to functional pools and to stabilization mechanisms. *Soil Biol. Biochem.* 39, 2183–2207.
- Walkley, A., Black, I.A., 1934. An examination of the Degtjareff method for determining soil organic matter, and a proposed modification of the chromic acid titration method. *Soil Sci.* 37, 29–38.
- Williams, P.C., Sobering, D.C., 1996. *How Do We Do it?: a Brief Summary of the Methods We Use in Developing Near Infrared Calibrations*. NIR Publications, Chichester, UK.
- Wise, B.M., Gallagher, N.B., Bro, R., Shaver, J.M., Windig, W., Koch, R.S., 2006. *Chemometric Tutorial for PLS\_Toolbox and Solo*. Eigenvector Research Inc., Wenatchee, WA, USA.
- Zimmermann, M., Leifeld, J., Fuhrer, J., 2007. Quantifying soil organic carbon fractions by infrared-spectroscopy. *Soil Biol. Biochem.* 39, 224–231.